PDF issue: 2025-07-11

Analysis and measurements for improved crank-line antennas

OKA, Tomohiro / NAKANO, Hisamatsu / YAMAUCHI, Junji / HIROSE, Kazuhide

Analysis and Measurements for Improved Crank-Line Antennas

H. Nakano, *Fellow, IEEE*, T. Oka, K. Hirose, *Member, IEEE*, and J. Yamauchi, *Member, IEEE*

Abstract—This paper describes the radiation characteristics of crank-line antennas radiating a circularly polarized wave. First, the radiation efficiency versus substrate permittivity is evaluated. Second, a 12-cell crank-line antenna of substrate permittivity $\varepsilon_r = 1$ and antenna height $B = \lambda_{11.85}/8$ is investigated as a reference antenna, where $\lambda_{11.85}$ is the wavelength at a frequency of 11.85 GHz. It is found that the main beam direction of the reference antenna varies $7°$ over a frequency range of approximately 6%, with an axial ratio of less than 3 dB and a gain of approximately 21 dB. Third, attention is paid to the gain behavior versus the antenna height. A way to increase the gain by modifying the antenna height is proposed. An increase of 1.5 dB from the gain of the reference antenna is demonstrated. Finally, the axial ratio, gain, and decoupling factor for crank-line antenna arrays are presented and discussed.

Index Terms—Antenna measurements, antenna theory.

I. Introduction

THERE has been increasing interest in radiation elements that radiate a circularly polarized (CP) wave over a relatively wide frequency range (for example, 5–12% for a 3-dB axial-ratio criterion). Such CP wave elements have been developed [1]–[3] and used for direct broadcasting satellite receiving antennas and mobile communication systems. The crank-line antenna [4] is one of these CP wave radiation elements.

The crank-line antenna is composed of many radiation cells. When the radiation cell dimensions [$2a, b$, and $c/2$ in Fig. 1(b)] are appropriately chosen, the crank-line radiates a CP wave. The concept and condition for CP wave radiation are discussed by Nishimura [5], [6] and Hall [7].

Experimental work on crank-line antennas that are printed on a dielectric substrate is found in [4]. The experimental results show that the crank-line antennas radiate a broadside CP wave beam with low sidelobes. The relationship between the broadside beam and the guided wavelength of the current along the crank lines is discussed in a recent study [8].

So far, the design of crank-line antennas has been dependent on experimental work and/or qualitative interpretations. To aid in the understanding and design of these antennas, detailed data on the radiation characteristics in which the mutual effects among the radiation cells are taken into account are required.

However, little data based on rigorous analysis are currently available.

The aim of this paper is to present the theoretical radiation characteristics of the crank lines, including the mutual effects among the radiation cells. For this, the method of moments (MoM) [9] is adopted. The radiation efficiency, radiation pattern, main beam direction, axial ratio, input impedance, and gain are evaluated on the basis of the numerically determined current distribution.

First, the effects of substrate permittivity on the radiation efficiency are investigated. A decrease in the radiation efficiency with an increase in the substrate permittivity is revealed. Second, a twelve-cell crank-line antenna of substrate permittivity $\varepsilon_r = 1$ and antenna height $B = \lambda_{11.85}/8$ ($\lambda_{11.85}$ is the free-space wavelength at 11.85 GHz) is chosen as a reference antenna and its radiation characteristics are analyzed. Third, the gain is investigated as a function of the antenna height. Modifying the antenna height from a certain point with a small flare angle (height modification) is proposed for increasing the gain.

Finally, two crank-line antenna arrays are presented—one is composed of two reference antennas and the other is composed of two crank-line antennas with height modification. The radiation characteristics of each array are evaluated as a function of the array-element spacing.

II. Configuration

Fig. 1(a) shows the coordinate system of a crank-line antenna where the crank arms 1 and 2, each made of a thin wire of radius ρ, are located on a dielectric substrate backed by an infinite conducting plane reflector. The substrate has thickness B and relative permittivity ε_r. The arm ends T_1 and T_2 are terminated in open circuits.

A radiation cell is composed of a bent line whose length is $2a + 2[b + (c/2)]$, as shown in Fig. 1(b). This length is chosen to be $2\lambda_g$ [6], where λ_g is the guided wavelength of the current along the crank arms. The number of radiation cells is designated as N_{cell}.

The crank arm 2 is shifted in the $+x$ and $-y$ directions by $s_x = a + (c/2)$ and $s_y = b + s_{\text{arm}}$, respectively, with respect to the crank arm 1, where s_{arm} is the spacing between the two crank arms. The currents along the two arms are generated by a balanced-type voltage source and set to be in phase at P_1 and P_2 using two detour lines, each having a length of $\delta = \lambda_g/4$.

The common configuration parameters throughout this paper are as follows: cell dimensions $2a = 3\lambda_g/4$, $b = \lambda_g/2$, and $c/2 = \lambda_g/8$, wire radius $\rho = 0.130$ mm $= 0.005\,14\lambda_{11.85}$,
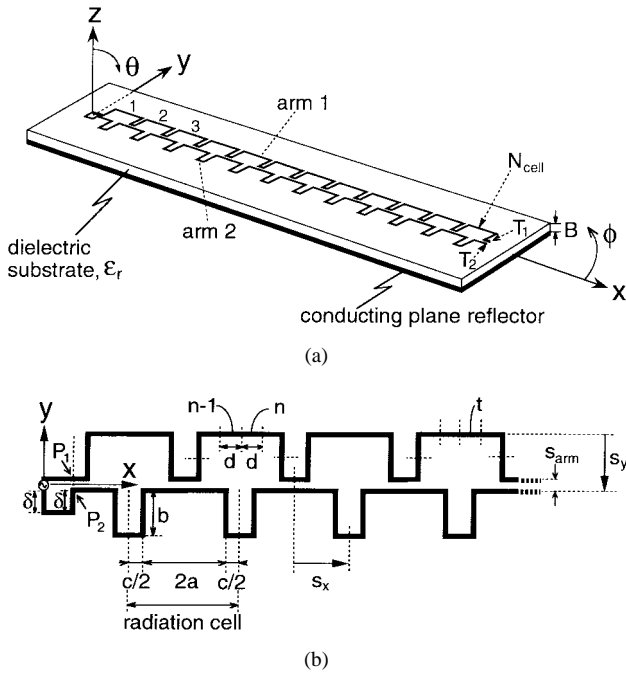
(a)

(b)

Fig. 1.   A crank-line antenna. (a) Coordinate system. (b) Radiation cells.

$N_{\text{cell}} = 12$, and $s_{\text{arm}} = \lambda_g/8$. The arm shifts are $s_x = \lambda_g/2$ and $s_y = 5\lambda_g/8$. Note that this s_x arm shift contributes to reduction of sidelobe levels [5].

III. ANALYSIS METHOD

The MoM [9] is used for analyzing the crank-line antenna. We assume that the crank line (wire) is perfectly conducting and that the dielectric substrate is lossless. It is also assumed that the wire radius of the crank line is small compared with the free-space wavelength so that the radiation characteristics can be calculated by only the current flowing in the wire axis direction.

The crank line is subdivided into $N+1$ segments of length d. The segments are labeled as $0, 1, 2, \cdots, n-1, n, \cdots, t, \cdots, N$, as shown in Fig. 1(b). The unknown current I on the crank line is expanded as $I = \sum_n I_n J_n$, where J_n $(n = 1, 2, \cdots, N)$ are expansion functions and I_n are unknown coefficients to be determined. In this paper, piecewise sinusoidal functions are used for the expansion functions.

The current distribution for a substrate of $\varepsilon_r \neq 1$ is determined using two Green's functions, $\Pi_{t,j}^x$ and $\Pi_{t,j}$, which are Sommerfeld-type integrals that include the effects of surface waves [10], while the current distribution for a substrate of $\varepsilon_r = 1$ is determined using the free-space Green's function [11], [12]. The radiation efficiency, radiation pattern, axial ratio, input impedance, and gain are evaluated on the basis of the numerically determined current distributions.

IV. RADIATION EFFICIENCY AND REFERENCE ANTENNA

A. Radiation Efficiency

We investigate the effects of the relative permittivity of a substrate ε_r on the radiation efficiency. The radiation
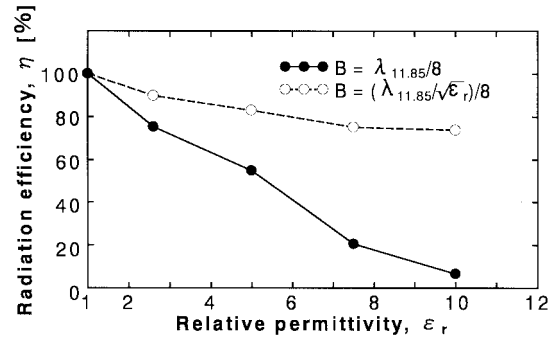

Fig. 2.   Radiation efficiency versus substrate permittivity.

efficiency η is defined as $(P_{\text{tot}} - P_{\text{sw}})/P_{\text{tot}}$, where P_{tot} is the total power input to the antenna and P_{sw} is the surface wave power. The radiation efficiency is given as $\eta = 1 - [\text{Re} \sum_n \sum_m I_m^* Z_{mn}^{\text{sw}} I_n]/[\text{Re} \sum_n \sum_m I_m^* (Z_{mn}^{\text{rd}} + Z_{mn}^{\text{sw}}) I_n]$, where I_m^* is the complex conjugate of I_m [13], [14]. Z_{mn}^{rd} and Z_{mn}^{sw} $(m = 1, 2, \cdots, N; n = 1, 2, \cdots, N)$ are the impedance matrix elements relating to the radiation field and surface-wave field components, respectively.

Fig. 2 shows the radiation efficiency η versus ε_r, where the antenna is designed using an approximated λ_g (as a function of ε_r) given by [15, (B.5)]. The solid line shows the case where the substrate thickness is kept constant; $B = \lambda_{11.85}/8 = 3.16$ mm. The radiation efficiency decreases as the relative permittivity ε_r increases. The dotted line shows the case where the substrate thickness is varied with ε_r; $B = (\lambda_{11.85}/\sqrt{\varepsilon_r})/8$. It is found that the radiation efficiency is approximately 90% and 74% for $\varepsilon_r = 2.6$ and 10, respectively.

When higher radiation efficiency (gain) is required, the substrate permittivity ε_r should be lower. In the following, an air substrate ($\varepsilon_r = 1, \eta = 100\%$) is chosen and the radiation characteristics are investigated in detail.

B. Reference Antenna

For $\varepsilon_r = 1$, the common configuration parameters expressed in terms of λ_g (mentioned in Section II) are simply expressed in terms of the free-space wavelength $\lambda_{11.85}$ at a test frequency of 11.85 GHz; $2a = 3\lambda_{11.85}/4 = 18.99$ mm, $b = \lambda_{11.85}/2 = 12.66$ mm, and $c/2 = \lambda_{11.85}/8 = 3.16$ mm. We choose the substrate thickness (antenna height) to be $B = \lambda_{11.85}/8 = 3.16$ mm and call this crank-line antenna the reference antenna.

From a practical point of view, we feed the crank-line antenna using a coaxial line, as shown in Fig. 3, where a quasi-tapered feed line is used. The quasi-tapered feed contributes to the antenna impedance matching over a relatively wide frequency range, as seen later. The parameters of the feed line are determined empirically; $f_a = 0.49$ mm, $f_b = 6.30$ mm, and $f_c = 4.75$ mm.

Calculations show that the current distributions of arms 1 and 2 are similar. Therefore, only the current distribution of arm 1 is shown in Fig. 4. The current flowing from input P_1 to the arm end T_1 exhibits traveling wave characteristics with attenuating amplitude. The phase progression implies that the guided wavelength is close to the free-space wavelength.
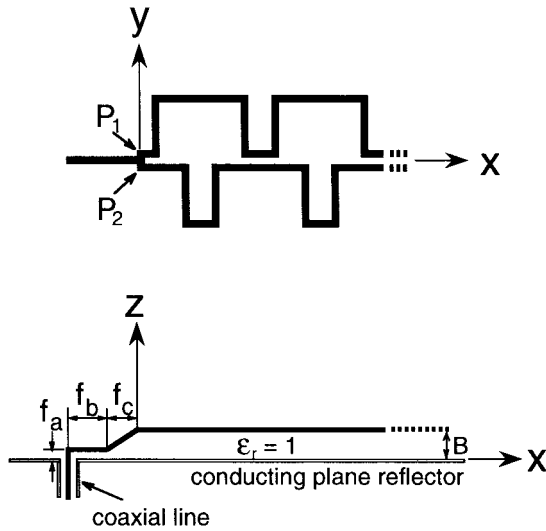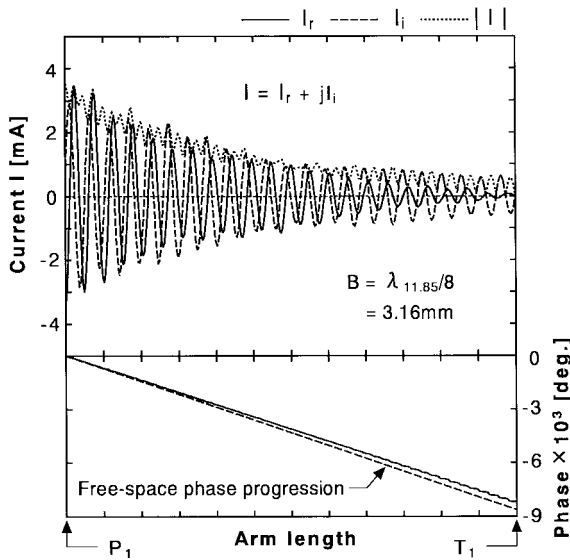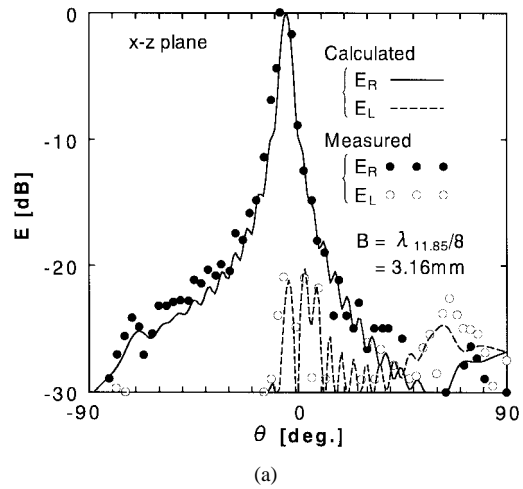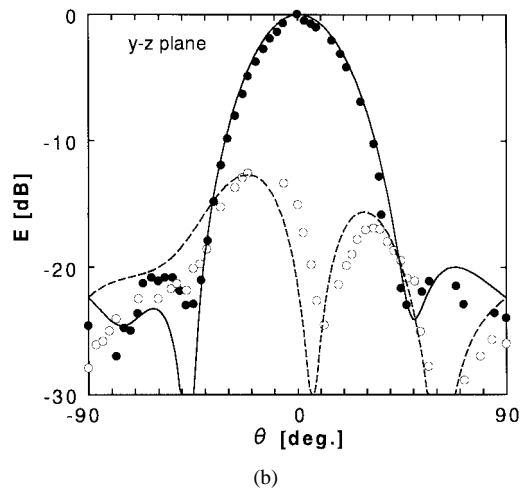
Fig. 3.   Coaxial line feed.

Fig. 4.   Current distribution of the reference antenna ($B = 3.16$ mm).

(a)

(b)

Fig. 5.   Radiation patterns of the reference antenna ($B = 3.16$ mm). (a) In the x-z plane. (b) In the y-z plane.

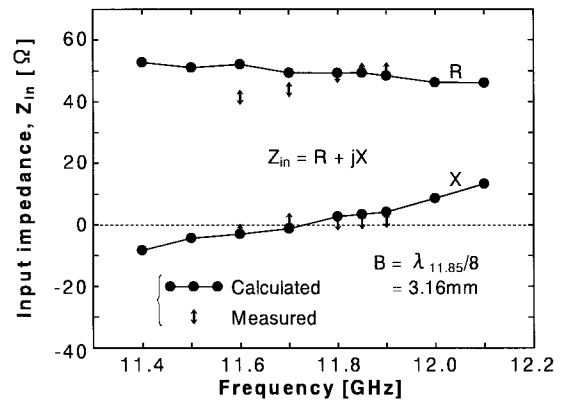Fig. 6.   Input impedance of the reference antenna ($B = 3.16$ mm).

The radiation fields calculated using the current distribution are presented in Fig. 5, where E_R and E_L are the radiation fields of right-hand circular polarization and left-hand circular polarization, respectively. The radiation pattern in the x-z plane has a sharp beam by virtue of the array effects of the radiation cells. The level of the cross-polarization component E_L in the x-z plane is low (-22 dB) in the main beam direction. For confirmation of the validity of the numerical results, the measured radiation fields are also presented. The numerical and measured radiation fields agree well.

The crank-line antenna is regarded as a traveling wave series-fed linear array composed of radiation cells [16]–[18]. This means that the main beam direction θ_0 varies as the frequency changes. The variation of the main beam direction is $7°$ from 11.4 to 12.1 GHz (approximately 6% bandwidth) over which the axial ratio of the main beam is less than 3 dB. The main beam has an almost constant gain of 21 dB and the input impedance is approximately 50 Ω, as shown in Fig. 6.

This input impedance is easily matched to the characteristic impedance of a conventional coaxial line.

V. ANTENNA HEIGHT

The radiation characteristics of the reference antenna are revealed in Section IV. In this section, we pay attention to the gain behavior as we change the antenna height of the reference antenna.
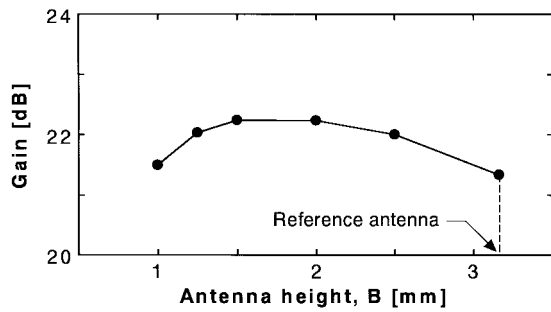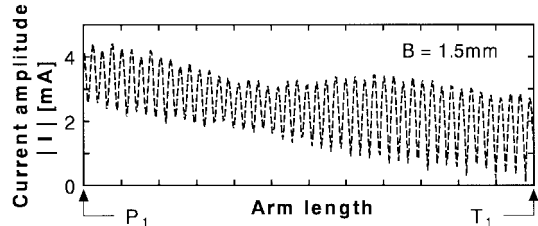
Fig. 7. Gain versus antenna height B.

Fig. 8. Current amplitude ($B = 1.5$ mm).

A. Small Antenna Height

When high gain is required, the current must be distributed over all of the radiation cells. This is achieved by making the antenna height smaller. Note that, as the antenna height becomes smaller, the attenuation of the current per radiation cell decreases, and the crank line exhibits transmission-line characteristics. This leads to an increase in the currents reflected from the arm ends (backward currents), resulting in generation of a cross-polarization field E_L.

Fig. 7 shows the gain variation at 11.85 GHz when the antenna height B is changed. The gain increases, as the antenna height is reduced from 3.16 mm (the height of the reference antenna). However, this tendency disappears when the antenna height is further reduced. A maximum gain of 22.2 dB is obtained at a height of $B = 1.5$ mm $\equiv B_{\text{GMAX}}$, which is approximately 1 dB higher than that of the reference antenna. This maximum gain is close to a value of 22.3 dB estimated using $G = 4\pi A/(\lambda_{11.85})^2$, where A is taken to be $12(2b + s_{\text{arm}})(2a + c)$.

Figs. 8 and 9 illustrate the current amplitude ($|I| = \sqrt{I_r^2 + I_i^2}$) and radiation pattern, respectively, for $B = B_{\text{GMAX}}$. The current is distributed over all the radiation cells, compared with that of the reference antenna (Fig. 4). However, the standing wave in the current distribution causes the cross-polarization field E_L off the main beam direction, as seen in Fig. 9. To further increase the gain, E_L should be suppressed. One way to realize this is to gradually change the antenna height from a certain point with a flare angle α, as shown in Fig. 10.

B. Flared Antenna Height

Fig. 10 shows an antenna-height modification, where the number of radiation cells which experience the gradual change in the height is designated as N_f.
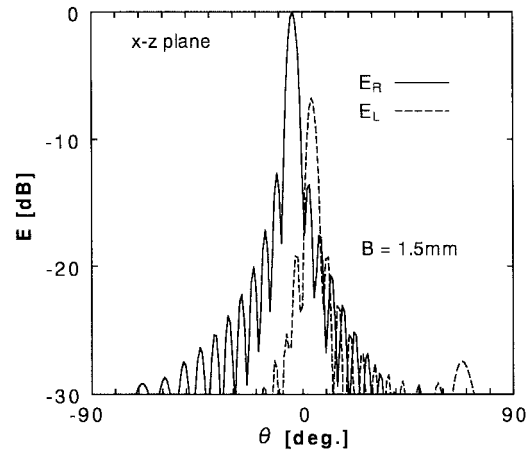
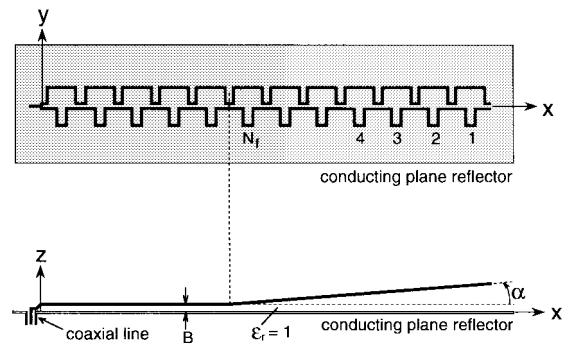Fig. 9. Radiation pattern in the x-z plane ($B = 1.5$ mm).
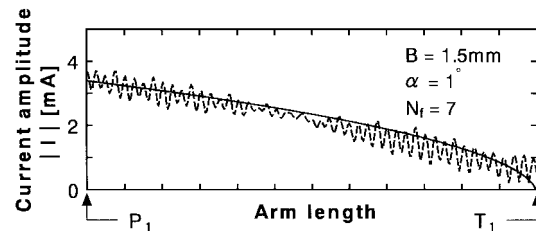
Fig. 10. Antenna height modification.

Fig. 11. Current amplitude ($N_f = 7, \alpha = 1°, B = 1.5$ mm).

We choose the flare angle and antenna height to be $\alpha = 1°$ and $B = 1.5$ mm, respectively (note that this height B is equal to B_{GMAX} mentioned in Fig. 7). Calculations show that as N_f increases, the standing wave observed in the current distribution becomes smaller and the gain increases. The gain reaches a maximum value at $N_f = 7$, which is approximately 0.5-dB higher than that at $N_f = 0$ (without the antenna-height modification). It should also be noted that this maximum gain is approximately 1.5-dB higher than that of the reference antenna.

The amplitude of the current distribution and the radiation pattern when the maximum gain is obtained are shown in Figs. 11 and 12, respectively. It is clear that the standing wave in Fig. 8 is reduced. As a result, E_L appearing in Fig. 9 is significantly reduced, while the main beam shape is almost the same.
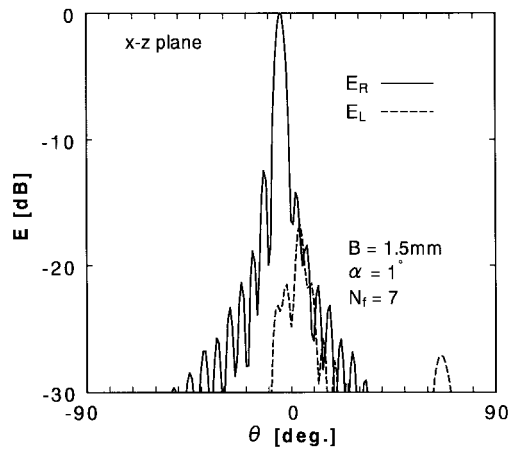
Fig. 12. Radiation pattern in the x-z plane ($N_f = 7, \alpha = 1°, B = 1.5$ mm).

The solid line in Fig. 11 shows the current amplitude obtained under the following assumptions: the radiation power from each radiation cell is equal and no reflected current from the arm end exists. The actual current amplitude is close to the solid line, leading to the enhanced gain.

We now investigate the frequency response of the radiation characteristics of the crank-line antenna with antenna-height modification parameters of $\alpha = 1°$ and $N_f = 7$. Fig. 13(a)–(c) show the main beam direction θ_0, axial ratio, and gain, respectively, when the frequency is changed. Note that the axial ratio and gain are evaluated in the main beam direction. The measured values are also presented.

For comparison, the main beam direction, axial ratio, and gain of the reference antenna are also depicted in Fig. 13. It can be said that antenna-height modification leads to an enhancement in the gain without significantly changing the main beam direction and axial ratio of the reference antenna.

Additional calculations show the following facts: the impedance bandwidth which gives a VSWR of less than 2 for a 50-Ω feed line is calculated to be approximately 29% for both the modified and reference antennas, and a 3-dB gain drop bandwidth in the fixed direction where the gain is maximum at a center frequency of 11.85 GHz does not show a significant difference between the modified and reference antennas (3.7% for the modified antenna and 4.2% for the reference antenna).

## VI. CRANK-LINE ANTENNA ARRAYS

The radiation characteristics of single crank-line antennas, including the mutual effects among the radiation cells, are revealed in the preceding sections. In this section, crank-line antenna arrays are analyzed using the MoM.

First, we analyze an array (shown in Fig. 14) where the reference antenna described in Section IV-B is used as the array element. Second, we analyze an array composed of two modified crank-line antennas, each having height modification parameters of $\alpha = 1°$ and $N_f = 7$. The radiation characteristics of the modified antenna are described in Section V-B.

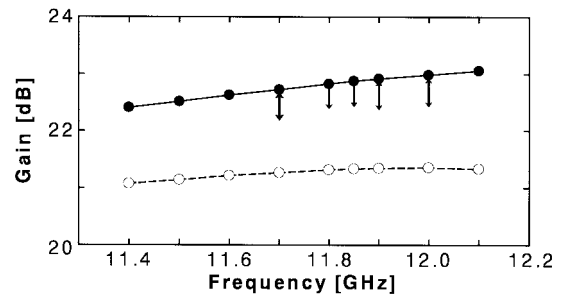As seen from Fig. 14, there are two conducting lines within the element spacing d_y and the shortest distance between
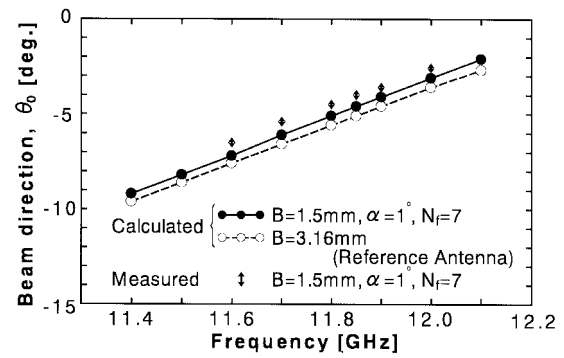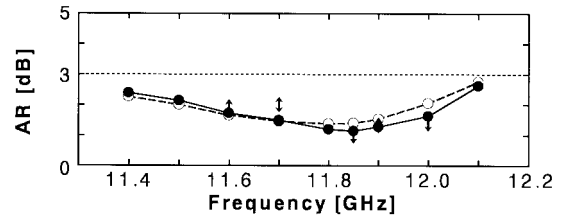
Fig. 13. Frequency responses. (a) Main beam direction. (b) Axial ratio. (c) Gain.

the neighboring lines is given as $d_y - 2(b + s_{arm}/2) = d_y - 1.125\lambda_{11.85}$. The dotted line in Fig. 15(a) shows the gain behavior of the array composed of the two reference antennas when d_y is changed. As d_y increases, the gain approaches a value of 24.3 dB, which is 3-dB higher than that of the single-reference antenna.

Axial ratio versus d_y for the array composed of the reference antennas is shown by the dotted line in Fig. 15(b). The axial ratio at $d_y \geq 1.2\lambda_{11.85}$ is approximately 1.4 dB, which is the inherent axial ratio of the reference antenna.

The mutual effects are elucidated by the decoupling factor (DCF) [19]. The DCF is defined as $20\log[|I_{in,1}|/|I_{in,2}|]$ [dB], where $I_{in,1}$ and $I_{in,2}$ are the currents at the input terminals of the array elements CL-1 and CL-2, respectively, under the following conditions: the input terminals of CL-1 are excited by a voltage source, with the input terminals of CL-2 loaded with the conjugate self-impedance of CL-2. A large DCF means that the mutual effects between the array elements are small.

The DCF for the array composed of the two reference antennas is calculated as a function of the element spacing d_y. It is found that a DCF of more than 20 dB is obtained at an element spacing of $d_y \geq 1.2\lambda_{11.85}$.
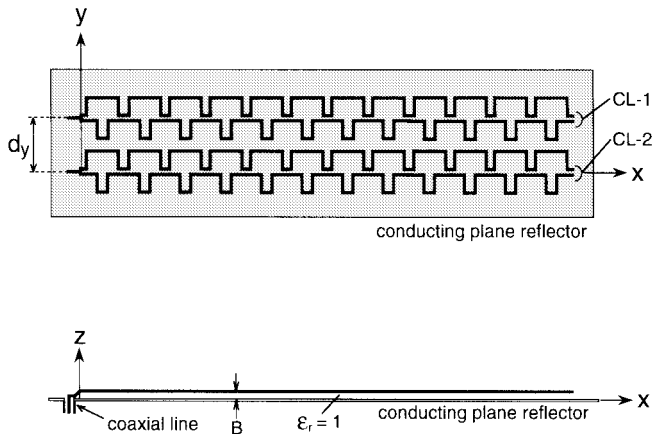
Fig. 14. Array of two crank-line antennas.

(a)

(b)

Fig. 15. Radiation characteristics of array antennas. (a) Gain versus element spacing. (b) Axial ratio versus element spacing.

The solid lines in Fig. 15 show the gain and axial ratio of the array composed of the two modified antennas with $\alpha = 1°$ and $N_f = 7$. The behavior of the gain and axial ratio as a function of d_y is similar to that for the array composed of the reference antennas. Calculations show that as d_y increases, the difference between the gains of the two arrays approaches 1.5 dB, which is the gain difference between the single-reference antenna and the single-modified antenna. Note that the DCF for the array composed of the two modified antennas is almost the same as that for the array composed of the two reference antennas; that is, the DCF is more than 20 dB at $d_y \geq 1.2\lambda_{11.85}$.
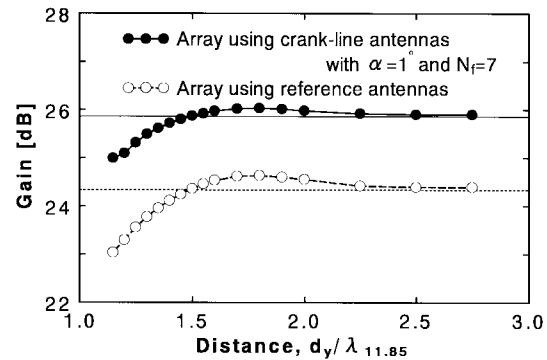
VII. CONCLUSION

The radiation characteristics of crank-line antennas are numerically evaluated using current distributions obtained by the MoM. A decrease in the radiation efficiency η with an increase in ε_r is revealed numerically. Taking this result into account, $\varepsilon_r = 1\,(\eta = 100\%)$ is chosen for realizing high gain in the subsequent analysis.
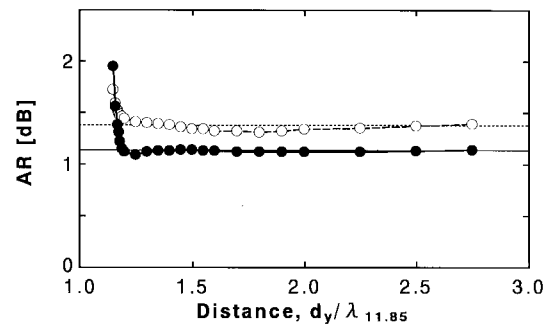
The radiation characteristics of a twelve-cell crank-line antenna of height $B = \lambda_{11.85}/8 = 3.16$ mm, used as a reference antenna, are revealed. The current distribution shows decaying traveling-wave characteristics. The main beam direction of the reference antenna varies $7°$ over a frequency range of approximately 6%, with an axial ratio of less than 3 dB and a gain of approximately 21 dB.

To reduce the cross-polarization field and obtain higher gain, the height of N_f radiation cells, starting with $B = 1.5$ mm, is gradually changed with a small flare angle α. It is found that the gain of a crank-line antenna with height-modification parameters of $\alpha = 1°$ and $N_f = 7$ is 1.5 dB higher than that of the reference antenna. It is also found that the frequency responses of the main beam direction and axial ratio of the crank-line antenna with height modification are similar to those of the reference antenna.

Finally, two crank-line arrays are investigated using the MoM; one is composed of two reference antennas and the other is composed of two modified crank-line antennas with $\alpha = 1°$ and $N_f = 7$. The gain, axial ratio, and DCF of each array are evaluated as a function of the spacing between the two array elements d_y. It is revealed that the axial ratio of each array reaches the inherent axial ratio of its corresponding array element at $d_y = 1.2\lambda_{11.85}$, with a DCF of more than 20 dB. It is also found that the axial ratio remains essentially constant for d_y greater than $1.2\lambda_{11.85}$.

As an alternative to height modification, further investigation should include flaring the length b of the radiation cell.

REFERENCES

[1] H. Nakano, H. Takeda, H. Mimaki, and J. Yamauchi, "Extremely low-profile helix radiating a circularly polarized wave," *IEEE Trans. Antennas Propagat.*, vol. 39, pp. 754–757, June 1991.
[2] H. Nakano, S. Okuzawa, K. Ohishi, H. Mimaki, and J. Yamauchi, "A curl antenna," *IEEE Trans. Antennas Propagat.*, vol. 41, pp. 1570–1575, Nov. 1993.
[3] K. Hirose and H. Nakano, "Dual-spiral slot antenna," *Proc. Inst. Elect. Eng.*, vol. 138, pt. H, no. 1, pp. 32–36, Feb. 1991.
[4] S. Nishimura, Y. Sugio, and T. Makimoto, "Crank-type circularly polarized microstrip line antenna," in *IEEE AP-S Int. Symp.*, Houston, TX, May 1983, pp. 162–165.
[5] S. Nishimura, A. Yamagata, A. Nishigaki, Y. Sugio, and T. Makimoto, "Circularly polarized microstrip line antenna," Tech. Rep. IEICE (Japan), 1986, vol. AP85-100, pp. 57–64.
[6] J. R. James and P. S. Hall, *Handbook of Microstrip Antennas.* London, U.K.: Peter Peregrinus, 1989, chs. 13, 14, 19.
[7] P. S. Hall, "Microstrip linear array with polarization control," *Proc. Inst. Elect. Eng.*, vol. 130, pt. H, pp. 215–224, Apr. 1983.

[8] H. Nakano and K. Hirose, "Numerical analysis of a crank-type antenna on a dielectric substrate," *Int. J. Microwave Millimeter-Wave Comput.-Aided Eng.*, vol. 4, no. 1, pp. 43–49, 1994.

[9] R. F. Harrington, *Fields Computation by Moment Methods*. New York: Macmillan, 1968.

[10] H. Nakano, S. Kerner, and N. G. Alexopoulos, "The moment method solution for printed wire antennas of arbitrary configuration," *IEEE Trans. Antennas Propagat.*, vol. 36, pp. 1667–1674, Dec. 1988.

[11] H. Nakano, M. Tanabe, J. Yamauchi, and L. Shafai, "Spiral slot antenna," in *Int. Conf. Antennas Propagat.*, New York, Mar. 1987, pp. 86–89.

[12] H. Nakano, *Analysis Methods for Electromagnetic Wave Problems*, E. Yamashita, Ed. Norwood, MA: Artech House, 1996, vol. 2, ch. 3.

[13] D. M. Pozar, "Considerations for millimeter wave printed antennas," *IEEE Trans. Antennas Propagat.*, vol. AP-31, pp. 740–747, Sept. 1983.

[14] M. Kominami and K. Rokushima, "On the numerical analysis of the microstrip printed dipoles," *Trans. IEICE*, vol. J69-B, no. 9, pp. 941–948, 1986 (Japan).

[15] I. J. Bahl and P. Bhartia, *Microstrip Antennas*. Norwood, MA: Artech House, 1980.

[16] J. D. Kraus, "A backward angle-fire array antenna," *IEEE Trans. Antennas Propagat.*, vol. AP-12, pp. 48–50, Jan. 1964.

[17] J. D. Kraus and K. R. Carver, "Wave velocities on the grid-structure backward angle-fire antenna," *IEEE Trans. Antennas Propagat.*, vol. AP-12, pp. 509–510, July 1964.

[18] J. D. Kraus, *Antennas*, 2nd ed. New York: McGraw-Hill, 1988, pp. 491–496.

[19] A. R. Stratori and E. J. Wilkinson, "An investigation of the complex mutual impedance between short helical array elements," *IRE Trans. Antennas Propagat.*, vol. 7, pp. 279–280, July 1959.

Tomohiro Oka was born in Kanagawa, Japan, on August 9, 1968. He received the B.E. and M.E. degrees from Hosei University, Tokyo, Japan, in 1991 and 1993, respectively.

He joined the Mitsubishi Co. Ltd., Tokyo, in 1993.

Mr. Oka is a member of the Institute of Electronics, Information and Communication Engineers of Japan.

Kazuhide Hirose (M'92) was born in Kanagawa, Japan, on September 18, 1959. He received the B.E., M.E., and Dr.E. degrees from Hosei University, Tokyo, Japan, in 1982, 1984, and 1991, respectively.

From 1984 to 1987, he was with Nihon Dengyo Kosaku Co., Ltd., Antenna Division, Tokyo, Japan. From 1991 to 1995, he was a Lecturer at Shonan Institute of Technology, Kanagawa, Japan. Since 1995, he has been a Faculty Member of Tokyo Denki University, Saitama, Japan, where he is an Associate Professor of electrical engineering. His research interests include printed antennas and slot antennas.

Dr. Hirose is a member of the Institute of Electronics, Information, and Communication Engineers of Japan.

Hisamatsu Nakano (M'75–SM'87–LF'92) was born in Ibaraki, Japan, on April 13, 1945. He received the B.E., M.E., and Dr.E. degrees in electrical engineering from Hosei University, Tokyo, Japan, in 1968, 1970, and 1974, respectively.

Since 1973, he has been a member of the faculty of Hosei University, Tokyo, Japan, where he is now a Professor of electronic informatics. His research topics include numerical methods for antennas, electromagnetic wave scattering problems, and light-wave problems. He was a Visiting Associate Professor at Syracuse University, NY (May through September 1981), where he worked on numerical analysis of electromagnetic coupling between wires and slots. He was also a Visiting Professor at University of Manitoba, Canada (March through September 1986), researching numerical techniques for analysis of microstrip antennas, and a Visiting Professor at University of California, Los Angeles (September 1986 to March 1987), working on microstrip line antenna analysis. He has published more than 120 refereed journal papers and 80 international symposium papers on antenna and relevant problems. He is the author of *Helical and Spiral Antennas* (New York: Wiley, 1987). In 1996, he published the chapter "Antenna analysis using integral equations," in the book *Analysis Methods of Electromagnetic Wave Problems—Volume II* (Norwood, MA: Artech House). He is also an Associate Editor of *IEEE Antennas and Propagation Magazine*. He has developed a parabolic antenna using backfire helical feed for direct reception of broadcasting satellite TV programs (DBS). He has also developed two types of small indoor flat DBS antennas using novel elements: curled and extremely low-profile helical elements. His other developments include microstrip antennas for global positioning systems (GPS), personal handy telephone antennas, and small dual-polarization Cassegrain antennas for direct reception of communication satellite TV programs.

Dr. Nakano was the recipient of an International Scientific Exchange Award from the Natural Sciences and Engineering Research Council of Canada. In 1987, he received the Best Paper Award of IEE Fifth International Conference on Antennas and Propagation. In 1994, he received the IEEE AP-S Best Application Paper Award (H. A. Wheeler Award).

Junji Yamauchi (M'85) was born in Nagoya, Japan, on August 23, 1953. He received the B.E., M.E., and Dr.E. degrees from Hosei University, Tokyo, Japan, in 1976, 1978, and 1982, respectively.

From 1984 to 1988, he served as a Lecturer at the Electrical Engineering Department of Tokyo Metropolitan Technical College, Japan. Since 1988, he has been a Faculty Member of Hosei University, where he is now a Professor of electronic informatics. His research interests include circularly polarized antennas and optical waveguides.

Dr. Yamauchi is a member of the Optical Society of America and the Institute of Electronics, Information, and Communication Engineers of Japan.